Chem

CellPress

Article

Ligand-enabled stereodivergence in nickel-catalyzed regioselective hydroboration of internal allenes

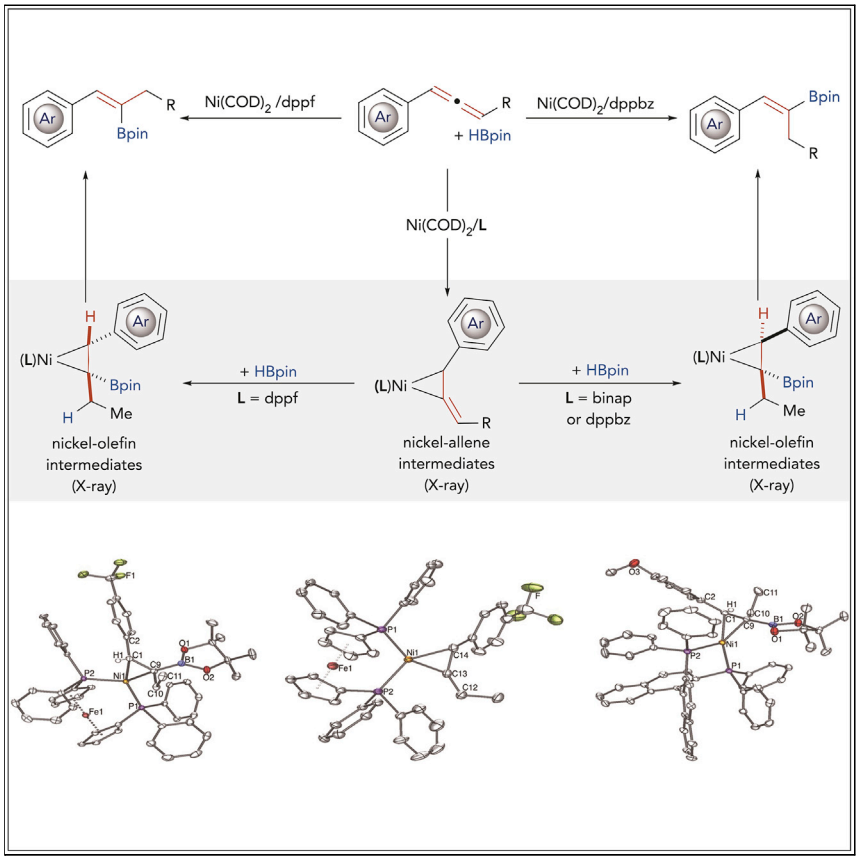

Stereodivergent synthesis of trisubstituted *Z*- and *E*-alkenylboronates has been developed through nickel-catalyzed regio- and stereoselective hydroboration of internal allenes. This protocol features good functional-group compatibility and broad substrate scope. In addition, several bisphosphine-ligated nickel-allene and nickel-olefin complexes have been synthesized, and their competence as reactive intermediates in the nickel-catalyzed allene hydroboration has been supported by a series of stoichiometric reactions and kinetic studies. Mechanistic studies suggest that the stereodivergence of this nickel-catalyzed allene hydroboration is controlled by steric properties of bisphosphine ligands.

Xiaoxu Yang, Chunchen Yuan, Shaozhong Ge

chmgsh@nus.edu.sg

Highlights

Regio- and stereoselective hydroboration of internal allenes

Stereodivergent synthesis of trisubstituted alkenylboronates

Isolation and characterization of nickel-allene and nickel-olefin intermediates

In-depth mechanistic and kinetic studies

Yang et al., Chem 9, 198–215
January 12, 2023
https://doi.org/10.1016/j.chempr.2022.10.003

CellPress

Chem

Article

Ligand-enabled stereodivergence in nickel-catalyzed regioselective hydroboration of internal allenes

Xiaoxu Yang,[1] Chunchen Yuan,[1] and Shaozhong Ge[1,2,*]

SUMMARY

Developing protocols for stereodivergent synthesis of multi-substituted alkenylboronates will simplify and unify the synthesis of *Z*- and *E*-stereoisomers of multi-substituted alkenes. Although tremendous efforts have been made to devise stereoselective approaches to access *Z*- or *E*-alkenylboronates, catalyst-controlled stereodivergence in their synthesis remains extremely rare. Herein, we demonstrate that such stereodivergence can be achieved for nickel-catalyzed hydroboration of internal allenes, which enables convenient synthesis of both stereoisomers of trisubstituted alkenylboronates from the same starting reagents. Mechanistic studies reveal that these nickel-catalyzed allene hydroboration reactions do not follow conventional hydrometallation or borylmetallation pathways with metal-hydride or metal-boryl intermediates. On the basis of the synthesis of potential nickel intermediates and their stoichiometric reactions, we propose new pathways for this nickel-catalyzed allene hydroboration, involving initial complexation of allenes to low-valent nickel catalysts followed by the stereo-determining reaction of bisphosphine-ligated nickel-allene intermediates with pinacolborane (HBpin) to form nickel-olefin compounds, which contain coordinated *Z*- or *E*-alkenylboronates.

INTRODUCTION

Acyclic trisubstituted (*E*)- and (*Z*)-alkenes are present in a wide range of natural products, pharmaceuticals, and organic materials and are also very useful starting materials for a variety of stereoselective chemical reactions.[1–3] The development of effective and selective protocols for the preparation of stereodefined trisubstituted alkenes is a longstanding and challenging task for chemical synthesis. Over the past decades, various selective approaches have been developed to synthesize trisubstituted alkenes, but most of these approaches are only effective for the synthesis of one stereoisomer, either *cis* or *trans*, of trisubstituted alkenes.[4–7] Different synthetic methods and starting materials are usually needed to synthesize both stereoisomers, and this potentially lowers the convenience and synthesis efficiency in cases where both stereoisomers are needed. Therefore, it will be more desirable to develop protocols that allow stereodivergent synthesis of both *cis*- and *trans*-trisubstituted alkenes from the same starting materials by just altering one reaction parameter such as ligands employed in metal-catalyzed reactions. Furthermore, compared with developing different methodologies for stereodivergent synthesis of different types of trisubstituted alkenes, it is more relevant to target stereodivergent synthesis of a family of trisubstituted alkene precursors because further stereospecific transformations will derivatize them into various types of other trisubstituted alkene products. In this regard, acyclic trisubstituted *Z*- and *E*-alkenylboronates will

THE BIGGER PICTURE

Stereodefined multi-substituted alkenylboronates are versatile reagents in organic synthesis and can serve as precursors to multi-substituted alkenes. The existing catalytic approaches to synthesizing such alkenylboronates are generally effective for their *Z*- or *E*-stereoisomer, and accessing both stereoisomers usually requires different synthetic methods or starting materials. Therefore, the development of stereoconvergent protocols for preparing both *Z*- and *E*-alkenylboronates from readily accessible starting reagents is highly desirable but challenging.

As reported here, we describe a convenient and effective protocol for preparing both stereoisomers of trisubstituted alkenylboronates by nickel-catalyzed regioselective stereodivergent hydroboration of internal allenes. This study also provides new mechanistic insights into nickel-catalyzed hydroboration reactions and could inspire chemists to develop other stereoselective hydrofunctionalization reactions of unsaturated hydrocarbons.

meet such needs because sp^2-alkenylboronates can undergo a variety of stereospecific transformations to furnish structurally diverse alkene products.[8]

Although numerous synthetic methodologies, such as boron-Wittig reaction,[9–11] lithiation/borylation of alkenyl halides,[12] Miyaura borylation of alkenyl halides,[13,14] hydroboration or carboboration of alkynes,[15–23] dehydrogenative borylation of alkenes,[24–27] isomerization of alkenylboronates,[28,29] and carbene insertion into B_2pin_2,[30] have been developed to prepare trisubstituted alkenylboronates, these approaches can provide access to only one stereoisomer, *E* or *Z*, of these alkenylboronates. Stereodivergent synthesis of both *Z*- and *E*-stereoisomers of trisubstituted alkenylboronates from the same starting reagents is extremely rare.[31,32] For example, lithiation-borylation or Miyaura borylation of alkenyl halides can be used to prepare both *Z*- and *E*-stereoisomers of trisubstituted alkenylboronates;[12–14] however, these transformations require pre-synthesis of stereodefined alkenyl halides. *cis*-Hydroboration of internal alkynes has been well established to prepare *Z*-alkenylboroantes,[33] but *trans*-hydroboration reactions to yield *E*-alkenylboronates are challenging and suffer from limited scope.[19–22] Very recently, stereoselective isomerization of *gem*-disubstituted alkenylboronates has been developed to access both stereoisomers of trisubstituted alkenylboronates,[31,32] but this isomerization protocol has an intrinsic limitation that one of the three substituents in alkenylboronate products has to be a methyl or silylmethyl group. Consequently, it still remains significant and highly desirable to develop effective and selective protocols for stereodivergent synthesis of stereodefined trisubstituted alkenylboronate compounds from readily accessible starting materials and commercially available base metal catalysts.

Allenes are organic molecules containing two cumulative C=C double bonds, and structurally diverse allenes can be efficiently and conveniently prepared nowadays by following well-established synthetic protocols.[34,35] Allenes are versatile reagents for chemical synthesis owing to high reactivity of their two orthogonal cumulative π-systems.[36–38] For example, allenes are useful starting materials to synthesize organoboron compounds,[39–47] and metal-catalyzed hydroboration of allenes is a well-known process that can produce allylboronate or alkenylboronate compounds, depending on the regioselectivity of the transformation.[48–53] Various transition metal catalysts have been identified for regioselective hydroboration of allenes with pinacolborane (HBpin), and the Bpin addition to either sp- or sp^2-hydridized carbon of the allene unit can be achieved with high regioselectivity (Figure 1A). One intriguing feature about these regioselective hydroboration reactions is that when the products containing an internal C=C double bond are formed, the reactions usually show very high stereoselectivity (often 99%–100%) and the products have a *Z*-configuration around the C=C double bond.[50–53] This *Z*-selectivity can be rationalized by considering hydrometallation or borylmetallation of one C=C double bond from the less-hindered side to minimize the steric repulsion between the catalyst and the substituent of the other C=C double bond (Figure 1B; one enantiomer of 1,3-disubstituted allene is drawn for illustrative purposes). This suggests that overriding the observed *Z*-selectivity may require to divert from hydrometallation and borylmetallation pathways.

In contrast to the well-developed *Z*-stereoselective hydroboration of allenes, the examples of *E*-stereoselective hydroboration of allenes with HBpin are extremely rare, and the pathways leading to the *E*-stereoselectivity are still subject to speculation. As far as we are aware, the only example of such *E*-stereoselective hydroboration is the copper-catalyzed hydroboration of allenes in the presence of CuCl and a

[1]Department of Chemistry, National University of Singapore, 3 Science Drive 3, Singapore 117543, Singapore

[2]Lead contact

*Correspondence: chmgsh@nus.edu.sg

https://doi.org/10.1016/j.chempr.2022.10.003

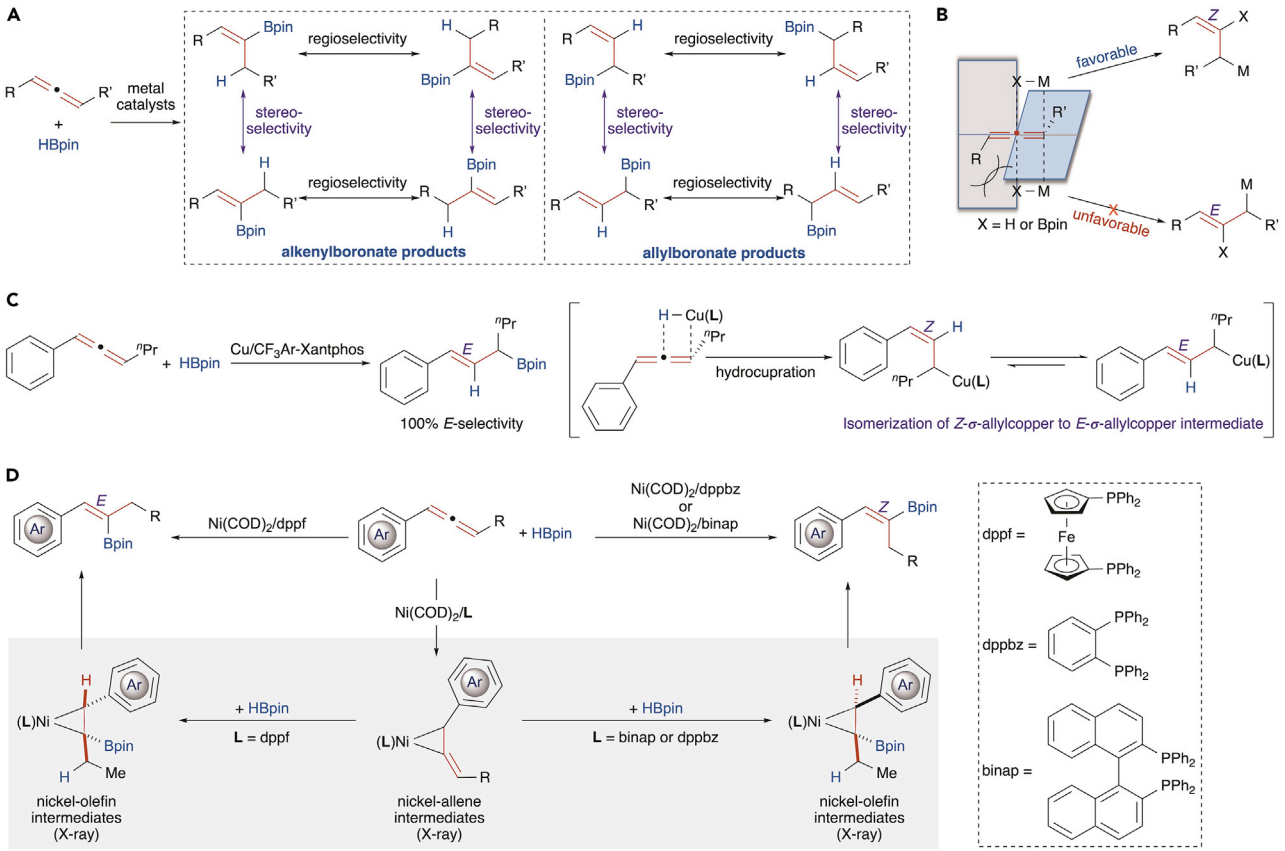

Figure 1. Hydroboration of internal disubstituted allenes with HBpin

(A) Regio- and stereoselectivity of metal-catalyzed hydroboration reactions of internal allenes.

(B) Allene hydrometallation and borylmetallation pathways leading to *Z*-stereoselectivity.

(C) Copper-catalyzed *E*-selective hydroboration of internal allenes to form *E*-allylboronates via *Z*-to-*E* isomerization of σ-allylcopper intermediates.

(D) Nickel-catalyzed stereodivergent hydroboration of internal allenes and potential bisphosphine-ligated nickel-allene and nickel-olefin intermediates.

xantphos-type ligand, and most of the selected allenes react with HBpin to form *E*-allylboronate products with 100% stereoselectivity.[49] For their copper-based catalyst system, Tsuji and coworkers proposed a pathway that involves isomerization of a *Z*-σ-allyl copper intermediate to an *E*-σ-allyl copper intermediate (Figure 1C). Nevertheless, this should lead to a thermodynamic mixture of *Z*- and *E*-allylboronates, unless the rate of this *Z*-to-*E* isomerization of σ-allyl copper intermediates is very fast or the rate of σ-bond metathesis between *Z*-σ-allyl copper species and HBpin is negligible in comparison with the rate of the corresponding reaction of *E*-σ-allyl copper intermediate. Except this copper-catalyzed *E*-selective hydroboration of allenes to form *E*-allylboronates, stereoselective hydroboration reactions of allenes to afford *E*-alkenylboronate products have not been identified.

During our continuous efforts to develop selective catalytic hydroboration of allenes,[50,53] we became intrigued by the prevalent *Z*-stereoselectivity observed for existing allene hydroboration reactions and thus intended to identify metal catalysts that could override such *Z*-stereoselectivity. Herein, we report a few nickel catalysts for both *Z*- and *E*-stereoselective hydroboration of disubstituted internal allenes (Figure 1D). These nickel catalysts enable convenient synthesis of both *Z*- and *E*-stereoisomers of a variety of trisubstituted alkenylboronate compounds. In

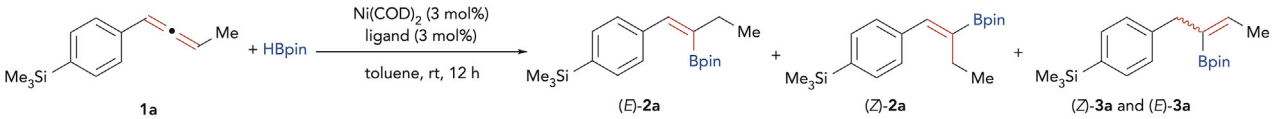

1a (*E*)-**2a** (*Z*)-**2a** (*Z*)-**3a** and (*E*)-**3a**

entry	ligand	conversion of **1a** (%)[a]	yield of **2a** (%)[a]	*E*/*Z* ratio of **2a**[a]	**2a**:**3a**[a]
1	dppp	<5	---	---	---
2	dcpe	<5	---	---	---
3	dppm	77	41	20:80	53:47
4	dppe	90	75	1:99	84:16
5	dppbz	95	85	1:99	89:11
6	binap	82	75	5:95	91:9
7	dppf	77	72	88:12	93:7
8[b]	dppbz	>99	90(85[c])	2:98	92:8
9[d]	dppf	>99	93(81[e])	97:3	94:6
10[b,f]	dppbz	80	72	4:96	92:8
11[d,f]	dppf	95	79	92:8	94:6

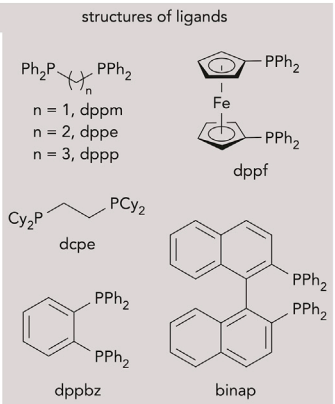

Figure 2. Evaluation of conditions for the nickel-catalyzed hydroboration of allene 1a with HBpin

Reaction conditions: allene **1a** (0.100 mmol), HBpin (0.120 mmol), $Ni(COD)_2$ (3.0 μmol), ligand (3.0 μmol), toluene (1 mL), room temperature, 12 h. [a]The values of conversion, yield of **2a**, *E*/*Z* ratio of **2a**, and ratio of **2a**:**3a** were determined by GC analysis with tridecane as internal standard. [b]1,4-Dioxane (1 mL) was used as the solvent. [c]The isolated yield of (*Z*)-**2a**. [d]Hexane (0.2 mL) was used as the solvent. [e]The isolated yield of (*E*)-**2a**. [f]$Ni(acac)_2$ was used instead of $Ni(COD)_2$.

addition, we also attempted to elucidate pathways for both *Z*- and *E*-selective hydroboration reactions with these nickel catalyst systems. Based on the detailed mechanistic studies, we propose new reaction pathways involving bisphosphine-ligated nickel(0)-allene intermediates, and the obtained *Z*- and *E*-selectivity can be rationalized by minimizing steric interaction between bisphosphine and boryl-containing allyl ligands in allylnickel intermediates. Mechanistic investigations include synthesis and characterization of potential organonickel intermediates, stoichiometric reactions of these organonickel complexes with reagents such as HBpin and allenes, identification of nickel species during and after hydroboration reactions, and deuterium-labeling experiments.

RESULTS AND DISCUSSION

Evaluation of conditions for the nickel-catalyzed hydroboration reaction of allene

We began our studies on the nickel-catalyzed hydroboration of allenes by evaluating nickel catalysts and conditions for the reaction of (4-(buta-1,2-dienyl-1-yl)phenyl)trimethylsilane **1a**, a 1,3-disubstituted allene, with HBpin. Nickel catalysts employed in this study were generated *in situ* by mixing $Ni(COD)_2$ with various bisphosphine ligands, and the results of the selected experiments are summarized in Figure 2. These reactions were conducted with allene **1a** as a limiting reagent in the presence of 3 mol % nickel catalyst at room temperature for 12 h. In general, this nickel-catalyzed hydroboration reaction of allene **1a** afforded four vinylboronate products (*Z*)-**2a**, (*E*)-**2a**, (*Z*)-**3a**, and (*E*)-**3a**, and the regio- and stereoselectivity of these reactions showed profound dependence on the bisphosphine ligands.

The reactions conducted with the nickel catalysts generated from $Ni(COD)_2$ and dppp or dcpe proceeded with very low conversion of allene **1a** (entries 1 and 2 in Figure 2). The reaction catalyzed by the combination of $Ni(COD)_2$ and dppm occurred with low regioselectivity and afforded a mixture of products **2a** and **3a** with a ratio of 53:47 (entry 3 in Figure 2). The reactions conducted by $Ni(COD)_2$ and dppe, dppbz,

or *rac*-binap occurred to high conversions of allene **1a** (entries 4–6 in Figure 2), yielding the (*Z*)-vinylboronate product (*Z*)-**2a** with high regioselectivity (84%–91%) and excellent stereoselectivity (95%–99%). In contrast, the reaction catalyzed by $Ni(COD)_2$ and dppf afforded (*E*)-vinylboronate (*E*)-**2a** with high regio- and stereoselectivity (entry 7 in Figure 2). We further improved the conversion, regioselectivity, and stereoselectivity of this reaction by evaluating various solvents for this transformation. For example, the reaction catalyzed by $Ni(COD)_2$ and dppbz in 1,4-dioxane afforded (*Z*)-**2a** in 85% isolated yield with 92% regioselectivity and 98% stereoselectivity (entry 8 in Figure 2), and the reaction catalyzed by $Ni(COD)_2$ and dppf in hexane produced (*E*)-**2a** in 81% isolated yield with 94% regioselectivity and 93% stereoselectivity (entry 9 in Figure 2). In addition, we also tested $Ni(acac)_2$, a bench-stable nickel salt, for the nickel-catalyzed stereodivergent hydroboration of **1a**, and these reactions proceeded to slightly lower conversions of **1a**, but with similarly high regio- and stereoselectivity (entries 10 and 11 in Figure 2), compared with the corresponding reactions conducted with $Ni(COD)_2$ (entries 8 and 9 in Figure 2).

Substrate scope

With the identified conditions and catalysts in hand, we explored the scope of 1,3-disubstituted allenes for these nickel-catalyzed stereodivergent hydroboration reactions, and the results are summarized in Figure 3. In general, a wide range of aryl,alkyl-disubstituted internal allenes (**1a**–**1z**) reacted smoothly with HBpin in hexane at room temperature in the presence of 3 mol % $Ni(COD)_2$ and dppf, affording the corresponding (*E*)-alkenylboronates ((*E*)-**2a**–(*E*)-**2z**) in modest to high isolated yields (51%–82%) with the *E*-selectivity ranging from 74% to 99%. In the meanwhile, hydroboration reactions of these allenes catalyzed by 3 mol % $Ni(COD)_2$ and dppbz in 1,4-dioxane produced the corresponding (*Z*)-alkenylboronates ((*Z*)-**2a**–(*Z*)-**2z**) in 57%–87% yields with the *Z*-selectivity ranging from 81% to 99%. In addition, diaryl- (**1aa**) and dialkyl-substituted internal allenes (**1ab** and **1ac**) also underwent these stereodivergent hydroboration reactions to afford stereodefined alkenylboronate products ((*E*)-**2aa**–(*E*)-**2ac**; (*Z*)-**2aa**–(*Z*)-**2ac**)) in 53%–82% isolated yields.

Data in Figure 3 show that the substitution pattern of aryl groups in aryl-substituted allenes does not have significant effect on the stereoselectivity of these nickel-catalyzed allene hydroboration reactions. For example, allenes containing a methyl group at the *para*-, *meta*-, and *ortho*-positions of the phenyl group reacted with similar stereoselectivity in the presence of $Ni(COD)_2$/dppf ((*E*)-**2b**, (*E*)-**2m**, and (*E*)-**2n**) or $Ni(COD)_2$/dppbz ((*Z*)-**2b**, (*Z*)-**2m**, and (*Z*)-**2n**). Nevertheless, the electronic property of the aryl groups in aryl-substituted allenes have profound but opposite influence on the stereoselectivity of the reactions catalyzed by $Ni(COD)_2$/dppf and $Ni(COD)_2$/dppbz. For example, allenes containing electron-deficient aryl groups ((*E*)-**2g** and (*E*)-**2l**) reacted with higher *E*-selectivity than allenes containing electron-rich aryl groups ((*E*)-**2h** and (*E*)-**2q**) in the presence of $Ni(COD)_2$/dppf; however, allenes containing electron-deficient aryl groups ((*Z*)-**2g** and (*Z*)-**2l**) reacted with lower *Z*-selectivity than allenes containing electron-rich aryl groups ((*Z*)-**2h** and (*Z*)-**2q**) in the presence of $Ni(COD)_2$/dppbz. In addition, the steric bulkiness of the alkyl substituents of allenes has noticeable influence on the stereochemistry outcome of $Ni(COD)_2$/dppf-catalyzed hydroboration reaction and the *E*-selectivity increased with the increasing steric bulkiness of the alkyl groups ((*E*)-**2b**, (*E*)-**2v**, and (*E*)-**2x**). However, such steric influence was negligible for the $Ni(COD)_2$/dppbz-catalyzed allene hydroboration (see (*Z*)-**2b**, (*Z*)-**2v**, and (*Z*)-**2x**).

These nickel-catalyzed stereodivergent hydroboration reactions show good functional tolerance, and various reactive groups, such as silyl (**2a**), fluoro (**2e**), chloro

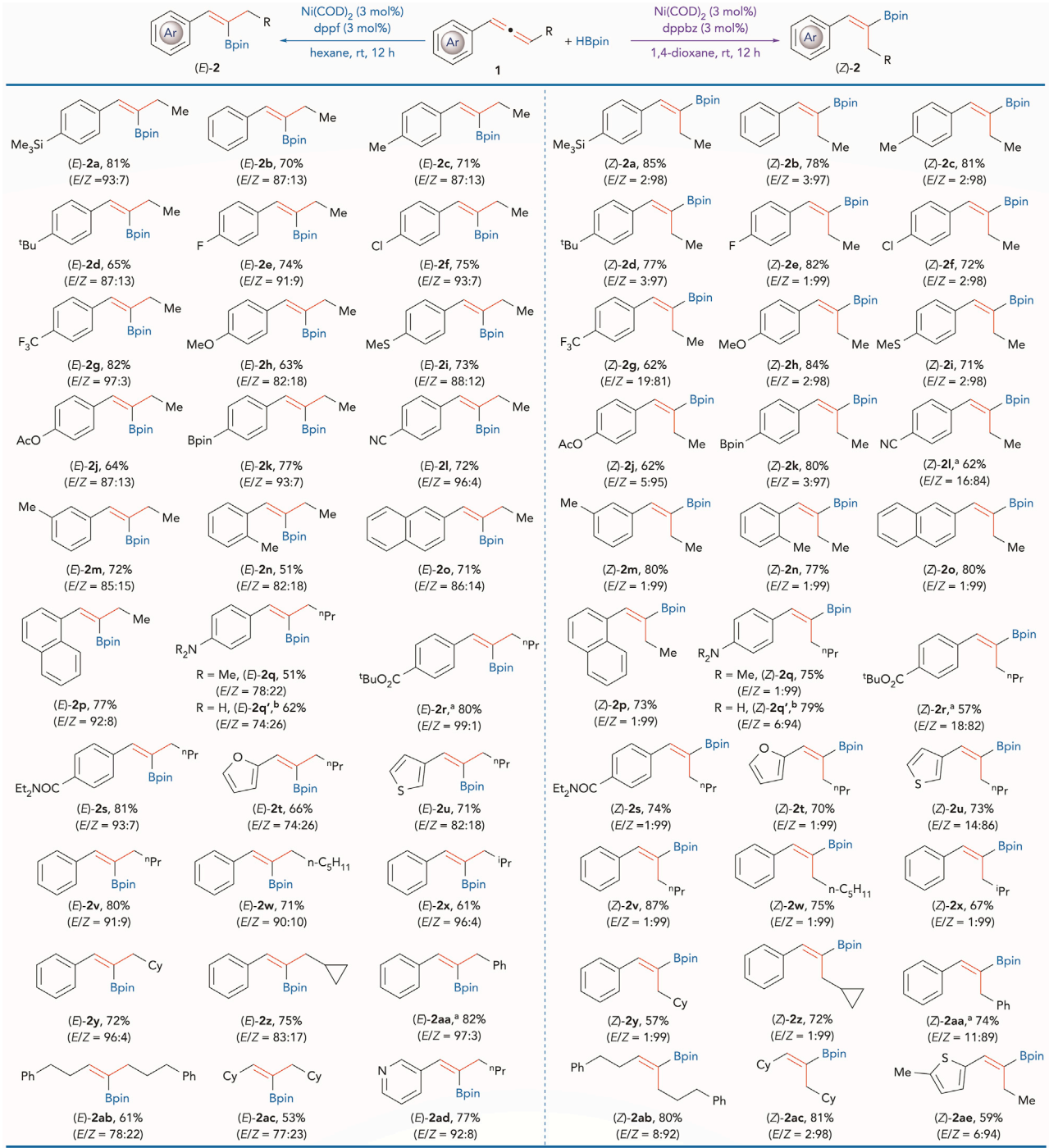

Figure 3. Scope of allenes for the nickel-catalyzed stereodivergent hydroboration reactions

Reaction conditions: allene (0.300 mmol), HBpin (0.360 mmol), $Ni(COD)_2$ (9.0 μmol), dppf or dppbz (9.0 μmol), hexane (0.6 mL) or 1,4-dioxane (3 mL), room temperature, 12 h, isolated yields after flash column chromatography on silica gel. The *E*/*Z* ratios of alkenylboronates **2a–2ae** were determined by gas chromatograph analysis on the crude mixtures of these reactions. [a]50°C. [b]HBpin (1.20 mmol).

(**2f**), trifluoromethyl (**2g**), ether (**2h**), sulfide (**2i**), carboxylic ester (**2j** and **2r**), boronic ester (**2k**), cyano (**2l**), tertiary amine (**2q**), primary amine (**2q′**), and amide (**2s**) moieties are compatible with the reaction conditions. In addition, allenes containing oxygen- and sulfur-heteroaromatic substituents also reacted under both sets of conditions

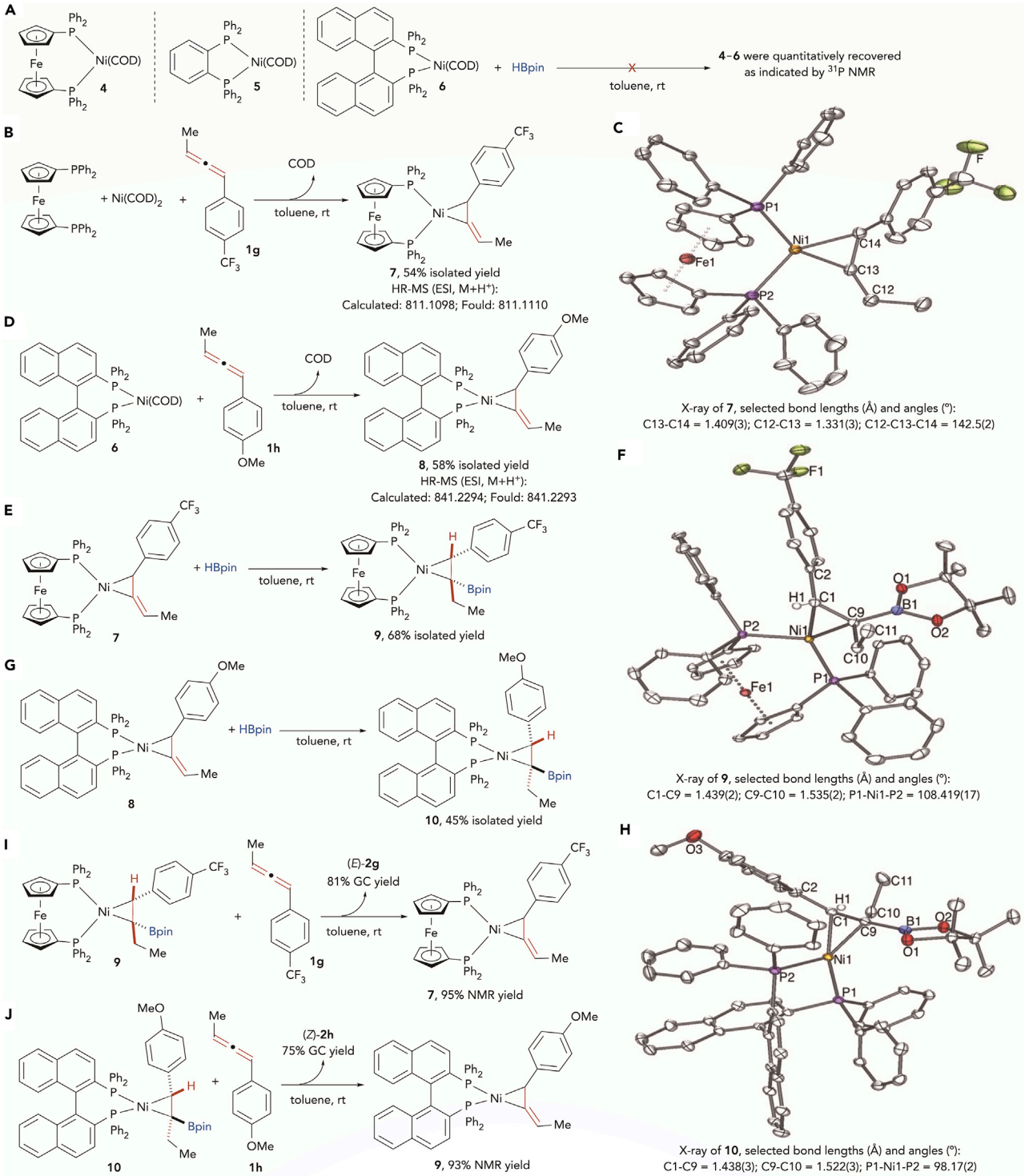

Figure 4. Stoichiometric reactions of potential bisphosphine-ligated nickel intermediates

(A) Reactions of nickel(0) complexes (**L**)Ni(COD) with HBpin.

(B) Synthesis of nickel-allene complex **7** by the reaction of $Ni(COD)_2$, dppf, and allene **1g**.

(C) X-ray structure of complex **7**.

(D) Synthesis of nickel-allene complex **8** by the reaction of (binap)Ni(COD) with allene **1h**.

(E) Synthesis of nickel-olefin complex **9** by the reaction of complex **7** with HBpin.

(F) X-ray structure of complex **9**.

Figure 4. *Continued*
(G) Synthesis of nickel-allene complex **10** by the reaction of complex **8** with HBpin.
(H) X-ray structure of **10**.
(I) Reaction of nickel-olefin complex **9** with allene **1g**.
(J) Reaction of nickel-olefin complex **10** with allene **1h**.

and afforded the desired alkenylboronate products ((*E*)-**2t** and (*E*)-**2u**; (*Z*)-**2t** and (*Z*)-**2u**) in good yields with high stereoselectivity. However, this stereodivergence could not be achieved for the nickel-catalyzed hydroboration of some 1,3-disubstituted allenes. For example, 3-pyridyl-substituted allene **1ad** underwent $Ni(COD)_2$/dppf-catalyzed hydroboration to form alkenylboronate (*E*)-**2ad** in 77% yield with 92% *E*-selectivity but could not react in the presence of $Ni(COD)_2$ and dppbz. Similarly, 2-thienyl-substituted allene **1ae** reacted in the presence $Ni(COD)_2$ and dppbz to afford alkenylboronate (*Z*)-**2ae** in 59% yield with 94% *Z*-selectivity but could not undergo $Ni(COD)_2$/dppf-catalyzed hydroboration reaction.

Isolation of nickel intermediates and their stoichiometric transformations

To obtain mechanistic insight into these nickel-catalyzed stereodivergent hydroboration reactions, we conducted a series of organometallic reactions to prepare several well-defined nickel compounds and evaluated their competence as reaction intermediates. We chose nickel catalysts generated from $Ni(COD)_2$ and three bisphosphine ligands (dppf, dppbz, and binap; entries 5–7 in Figure 2) to carry out these mechanistic investigations. The combination of $Ni(COD)_2$ and bisphosphine ligand (**L**) is one of the most commonly used approaches to generate nickel(0) catalyst precursors and has been practiced in countless nickel-catalyzed organic reactions.[54,55] It is commonly accepted that the coordination of a bisphosphine ligand with $Ni(COD)_2$ forms (**L**)Ni(COD), which then reacts with substrates to enter the catalytic cycles.[56,57] For these nickel-catalyzed hydroboration reactions, the initial step should be the reaction of nickel(0) species with allenes or HBpin. In general, there are two scenarios for this initial step: (1) bisphosphine-ligated nickel(0) complexes (**L**)Ni(COD) (**L** = dppf [**4**]; **L** = dppbz [**5**]; and **L** = binap [**6**]), generated from the reaction between $Ni(COD)_2$ and bisphosphine ligands, react with allenes or HBpin, or (2) $Ni(COD)_2$ reacts first with allenes or HBpin, and subsequent ligation by bisphosphines occurs. Both reaction sequences are evaluated for the reactions of nickel(0) complexes with HBpin or allenes.

Oxidative addition of HBpin to phosphine-ligated nickel(0) complexes to form (**L**)Ni(H)(Bpin) has been proposed as one key step in nickel-catalyzed hydroboration of unsaturated hydrocarbons.[52,58] However, the reactions of nickel(0) complexes (**L**)Ni(COD) (**4**–**6**) with HBpin on NMR scales did not occur as indicated by ^{31}P NMR spectroscopic analysis, and these nickel(0) complexes were recovered quantitatively (Figure 4A). In addition, we also conducted the reactions of $Ni(COD)_2$ and HBpin with subsequent addition of bisphosphine ligands (dppf, dppbz, or binap), and these reactions produced bisphosphine-ligated nickel(0) complexes (**L**)Ni(COD) (**4**–**6**) with high selectivity. The results of these reactions suggest that oxidative addition of HBpin to $Ni(COD)_2$ in the presence of bisphosphine ligands or to bisphosphine-ligated nickel(0) complexes (**L**)Ni(COD) is unlikely the initiation step in these nickel-catalyzed hydroboration reactions of allenes.

We then conducted the reactions of (**L**)Ni(COD) (**4**–**6**) with allenes. An NMR-scale reaction of (dppf)Ni(COD) (**4**) with allene **1g** in C_6D_6 went to completion in 10 min and revealed the formation of a new nickel species with ^{31}P NMR resonances at δ 31.7 and 22.1 ppm (d, $^2J_{pp}$ = 21.3 Hz). This new nickel complex could also be obtained in 54% yield by the three-component reaction of $Ni(COD)_2$, dppf, and allene **1g** in

toluene (Figure 4B). Single-crystal X-ray diffraction analysis on the isolated material (Figure 4C) confirmed its identity as a nickel-allene complex **7**. The geometry around the nickel center in compound **7** is nearly square planar (the sum of four adjacent angles around the nickel center is 359.95°), and its coordinated allene moiety significantly deviates from the linear structure as indicated by the angle C12-C13-C14 of 142.5(2)°. In addition, the coordinated C=C double bond (C13-C14 = 1.409(3) Å) of its allene unit is significantly elongated than the uncoordinated double bond (C12–C13 = 1.331(3) Å). All these structural features suggest that the nickel center in complex **7** is oxidized to certain degrees.

The reactions of (dppbz)Ni(COD) (**5**) with several allenes were attempted on NMR scales, and no new nickel species were detected by ^{31}P NMR analysis with nearly quantitative recovery of nickel complex **5**. The different reactivity of (dppf)Ni(COD) (**4**) and (dppbz)Ni(COD) (**5**) toward allenes likely stems from the different steric properties of dppf and dppbz ligands. Both (dppf)Ni(COD) (**4**) and (dppbz)Ni(COD) (**5**) are 18e complexes, and the substitution of COD ligand with allenes requires partial or complete dissociation of COD from these two nickel complexes. The relatively larger size of dppf ligand compared with dppbz ligand makes the coordination of COD in (dppf)Ni(COD) (**4**) weaker than the coordination of COD in (dppbz)Ni(COD) (**5**), as can be seen from the longer average distance between nickel and the coordinated carbon atoms of COD ligand in (dppf)Ni(COD) (2.128(2) Å)[55] than in (dppbz)Ni(COD) (2.1067(13) Å; see the supplemental information for its X-ray structure). This relatively weaker coordination of COD to the nickel center in (dppf)Ni(COD) (**4**) enables facile ligand substitution of COD with allenes in (dppf)Ni(COD).

We subsequently carried out the three-component reaction of Ni(COD)$_2$, dppbz, and allene **1h** on an NMR scale in C_6D_6. This reaction selectively formed (dppbz)$_2$Ni, and (dppbz)Ni(COD) was not detected during the course of the reaction as monitored by ^{31}P NMR spectroscopic analysis. For comparison, we also conducted an NMR-scale reaction of Ni(COD)$_2$ and dppbz in C_6D_6, and this reaction afforded a mixture of (dppbz)Ni(COD) and (dppbz)$_2$Ni in a ratio of 86:14. The results of these two reactions suggest that allene **1h** reacts first with Ni(COD)$_2$ to form a COD-free allene-ligated nickel(0) species, which then reacts with dppbz to form (dppbz)$_2$Ni. Indeed, an NMR-scale reaction of Ni(COD)$_2$ with allene **1h** in C_6D_6 showed that the ^{1}H NMR resonances of Ni(COD)$_2$ completely disappeared upon mixing and uncoordinated COD was detected. However, nickel(0) complexes containing only allene ligands are configurationally unstable and could not be isolated in the absence of phosphine ligands.[59] In addition, the propensity for the formation of (dppbz)$_2$Ni complex in the three-component reaction of Ni(COD)$_2$, dppbz, and allene **1h** precludes the observation of nickel(0)-allene complexes ligated by dppbz, and this poses additional challenge to study the mechanism of the nickel-catalyzed *Z*-selective allene hydroboration. Therefore, we chose to study the stoichiometric reactions with other nickel systems that can catalyze *Z*-selective allene hydroboration to illustrate the pathways for the formation of (*Z*)-alkenylboronates.

As shown in Figure 2 (entry 6), the nickel complex generated from Ni(COD)$_2$ and binap could also catalyze *Z*-selective hydroboration of allenes, and we then chose this nickel system to synthesize potential nickel intermediates to illustrate the pathways for the *Z*-selective allene hydroboration. The NMR-scale reaction of (binap)Ni(COD) (**6**) with allene **1h** in toluene showed the formation of a new nickel species with broad ^{31}P NMR resonances at δ 39.0 and 26.8 ppm ($^2J_{PP}$ was not resolved as a result of fluxionality in toluene at 25°C; $^2J_{PP}$ = 42.8 Hz at 0°C) (Figure 4D). This new nickel complex is thermally labile, and the attempt to isolate it in pure form led to its partial

decomposition. However, mass spectroscopic and two-dimensional NMR spectroscopic analysis on the isolated material confirmed its identity as binap-ligated nickel-allene complex **8**, as shown in Figure 4D (see Figures S1–S4). Complex **8** could also be prepared in a similar yield by the three-component reaction of $Ni(COD)_2$, binap, and allene **1h**. In addition, we found that this three-component reaction went to completion upon mixing, but the reaction of $Ni(COD)_2$ with binap to form (binap)Ni(COD) (**6**) was rather slow and required 20 h to complete. This indicates that (binap)Ni(COD) is not a kinetically competent nickel intermediate for this three-component reaction to form nickel complex **8**, although (binap)Ni(COD) could react with allene **1h** to produce complex **8**. Considering the above-mentioned fast ligand exchange between $Ni(COD)_2$ and allene **1h**, we propose that, in this three-component reaction, $Ni(COD)_2$ first reacts with allene **1h** to form an allene-ligated nickel(0) intermediate, which then reacts with binap to afford binap-ligated nickel-allene complex **8**.

With well-defined nickel-allene complexes **7** and **8** in hand, we evaluated their reactivity with HBpin. The reaction of complex **7** with HBpin on an NMR scale yielded a new nickel species with ^{31}P NMR resonances at δ 27.2 and 24.2 ppm (d, $^2J_{PP}$ = 27.1 Hz). This new nickel compound was formulated as compound **9** and was isolated in 68% yield (Figure 4E). The X-ray analysis on the isolated material (Figure 4F) shows that it is a nickel-olefin complex with a coordinated alkenylboronate (*E*)-**2g**. Similarly, binap-ligated nickel-allene complex **8** also reacted with HBpin to afford nickel-olefin complex **10**, which contains a coordinated alkenylboronate (*Z*)-**2h**, in 45% isolated yield (Figure 4G), and the molecular structure of compound **10** was also confirmed by single-crystal X-ray analysis (Figure 4H). The ^{31}P NMR resonances of complex **10** are found at δ 33.0 and 25.9 ppm (d, $^2J_{PP}$ = 46.6 Hz).

The geometry around the nickel center in nickel-olefin compounds **9** and **10** is approximately square planar, and the bond lengths of the coordinated double bonds (C1–C9 = 1.439(2) Å for compound **9** and C1–C9 = 1.438(3) Å for compound **10**) are between bond lengths of a typical C=C double bond (1.34 Å) and a typical C–C single bond (1.53 Å).[60] The *para*-trifluoromethylphenyl and Bpin groups in compound **9** are on the same side of the nickelocyclopropane ring, and differently, the *para*-methoxyphenyl and Bpin groups in complex **10** are on the different sides of the nickelocyclopropane ring. The P1-Ni1-P2 angle is 108.419(17)° for complex **9** and 98.17(2)° for complex **10**, which shows that dppf ligand is sterically more hindered than binap ligand. In addition, the coordinated alkenylboronate (*E*)-**2g** in complex **9**, with the two big groups of aryl and Bpin on the same side of its double bond, is sterically less demanding than the coordinated alkenylboronate (*Z*)-**2h** in complex **10**, with the two big groups of aryl and Bpin on the different sides of its double bond. This combination of dppf and (*E*)-**2g** in **9** or binap and (*Z*)-**2h** in complex **10** is to minimize the steric interaction between the bisphosphine and olefin ligands. Therefore, the conversion of the nickel-allene intermediate with HBpin to the nickel-olefin intermediate is the stereo-determining step for these nickel-catalyzed stereodivergent hydroboration reactions, and the steric difference between dppf and binap likely controls the stereochemistry of the alkenylboronate products.

The reaction between dppf-ligated nickel-alkene complex **9** and allene **1g** proceeded smoothly at room temperature and afforded nickel-allene complex **7** in 95% NMR yield and alkenylboronate (*E*)-**2g** in 81% GC yield (Figure 4I). Similarly, binap-ligated nickel-alkene compound **10** reacted with allene **1h** to form nickel-allene complex **8** in 93% yield with the concomitant release of alkenylboronate (*Z*)-**2h** in 75% GC yield (Figure 4J).

Identity of nickel species in the catalytic reaction mixture and kinetic studies

To identify nickel intermediates in these nickel-catalyzed stereodivergent hydroboration reactions, we monitored by ^{31}P NMR spectroscopy the hydroboration reactions of allenes **1g** and **1h** in the presence of 10 mol % Ni(COD)$_2$/dppf and Ni(COD)$_2$/binap, respectively. During the conversions of allene **1g** and **1h**, bisphosphine-ligated nickel-olefin complexes **9** and **10** were observed as major nickel intermediates. In addition, nickel complexes **9** and **10** could be converted to the desired alkenylboronate products by the reaction with allenes (Figures 4I and 4J), suggesting that bisphosphine-ligated nickel-olefin complexes are on-cycle resting states of nickel catalysts for these nickel-catalyzed allene hydroboration reactions.

The kinetic behaviors of the nickel-catalyzed hydroboration of allenes were subsequently assessed to understand the turnover limiting steps of these stereodivergent reactions. We measured the dependence of initial rates of the hydroboration on the concentrations of the nickel catalyst, allene, and HBpin. To make initial rates valid for kinetic analysis, we chose well-defined nickel-allene or nickel-olefin complexes as the source of nickel to eliminate the process to generate active nickel intermediates from bisphosphine ligand and Ni(COD)$_2$. In addition, kinetic experiments of hydroboration reactions were conducted in THF because all reagents are soluble in THF.

Kinetic studies for the *E*-selective allene hydroboration were performed with the reaction of allene **1g** with HBpin catalyzed by nickel-allene complex **7** in THF at room temperature (Figure 5A). The initial rate of this *E*-selective hydroboration reaction was determined by measuring the formation of alkenylboronate (*E*)-**2g** with respect to time. The plots of concentrations of (*E*)-**2g** versus time at various concentrations of complex **7**, allene **1g**, and HBpin are shown in Figures S28–S33. The plots of initial rates versus the concentrations of the catalyst, allene, and HBpin are shown in Figure 5A. The results of these kinetic experiments revealed that this nickel-catalyzed *E*-selective hydroboration is first order in the nickel catalyst, zero order in allene, and zero order in HBpin.

Kinetic behaviors for the *Z*-selective allene hydroboration were evaluated with the reaction of allene **1h** with HBpin catalyzed by nickel-olefin complex **10** in THF at room temperature (Figure 5B). The initial rate of this *Z*-selective hydroboration reaction was determined by measuring the formation of alkenylboronate (*Z*)-**2h** with respect to time. The plots of concentrations of (*Z*)-**2h** versus time at various concentrations of complex **10**, allene **1h**, and HBpin are shown in Figures S34–S39. The plots of initial rates versus the concentrations of the catalyst, allene, and HBpin are shown in Figure 5B. The results of these kinetic experiments revealed that this nickel-catalyzed *Z*-selective hydroboration is also first order in the nickel catalyst, zero order in allene, and zero order in HBpin.

Overall mechanism of nickel-catalyzed stereodivergent allene hydroboration

Based on the results of stoichiometric reactions of organonickel intermediates and kinetic experiments, we proposed a plausible mechanism for the nickel-catalyzed regiodivergent hydroboration of internal allene **1** (Figure 6A). Ligand exchange reaction between Ni(COD)$_2$ and allene **1** generates allene-ligated nickel(0) species Ni(allene)$_n$, which then reacts with bisphosphine ligand **L** to form a bisphosphine-ligated nickel-allene complex **i**. The σ-bond metathesis between nickel intermediate **i** and HBpin affords an η^1-allyl nickel intermediate **ii**,[61] and the subsequent ligand-controlled σ-π-σ isomerization of η^1-allyl nickel intermediate **ii** to **iv** or **vii** through η^3-allyl nickel species **iii** or **vi**, respectively, defines the stereochemistry outcome of alkenylboronate products. When a sterically demanding dppf ligand, with a bite angle of 108.419(17)°, derived the crystallographic data of nickel complex **9**, is employed, the σ-π-σ isomerization of **ii**-**iii**-**iv** takes place in a way that positions the aryl and Bpin groups on the

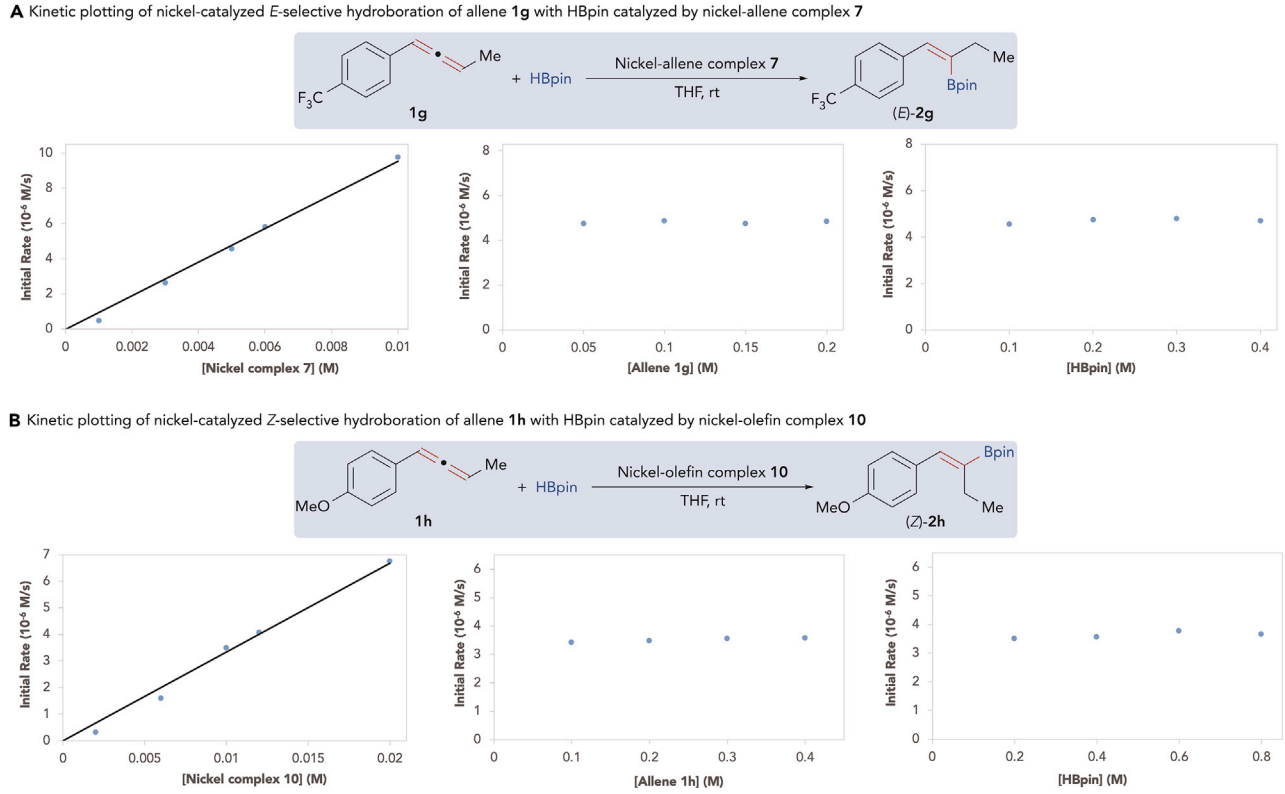

Figure 5. Kinetic profiles for nickel-catalyzed hydroboration reactions of allenes

(A) Plots of initial rates versus concentrations of catalyst, allene, and HBpin for hydroboration of allene **1g** with HBpin catalyzed by dppf-ligated nickel-allene complex **7**.

(B) Plots of initial rates versus concentrations of catalyst, allene, and HBpin for and hydroboration of allene **1h** with HBpin catalyzed by binap-ligated nickel-alkene complex **10**.

same side of C=C double bond of η^1-allyl nickel intermediate **iv** (the left cycle in Figure 6A). When a sterically less-hindered binap ligand, with a bite angle of 98.17(2)° derived the crystallographic data of nickel complex **10**, is utilized, the σ-π-σ isomerization **ii**-**vi**-**vii** occurs in a way that places the aryl and Bpin groups on the different sides of C=C double bond of η^1-allyl nickel intermediate **vii** (the right cycle in Figure 6A). The C–H reductive elimination from nickel species **iv** and **vii** with the concomitant coordination of their C=C double bonds to the nickel center forms nickel-olefin complexes **v** and **viii**, respectively. The dissociation of alkenylboronate products (*E*)-**2** and (*Z*)-**2** from nickel-olefin complexes **v** and **viii**, respectively, forms sterically unsaturated nickel intermediates (L)Ni(0), which then react with allene **1** to regenerate the catalytically active nickel-allene complexes **i** to close the catalytic cycles. Nickel-olefin complexes as the catalyst resting state and the observed first-order rate dependence only on nickel catalysts indicate that the dissociation of alkenylboronate products from nickel-olefin intermediates to form (L)Ni(0) is the turnover-limiting step for the nickel-catalyzed stereodivergent allene hydroboration.

To provide further experimental evidence to support the proposed pathways for this nickel-catalyzed hydroboration reaction, we conducted a series of control reactions and deuterium-labeling experiments. For example, we monitored by ^{31}P NMR spectroscopy Ni(COD)$_2$/binap-catalyzed hydroboration reaction of allene **1h** in the presence of an equal molar amount of alkenylboronate (*Z*)-**2o** (Figure 6B) and Ni(COD)$_2$/binap-catalyzed hydroboration reaction of a 1:1 mixture of allene **1h** and **1o**

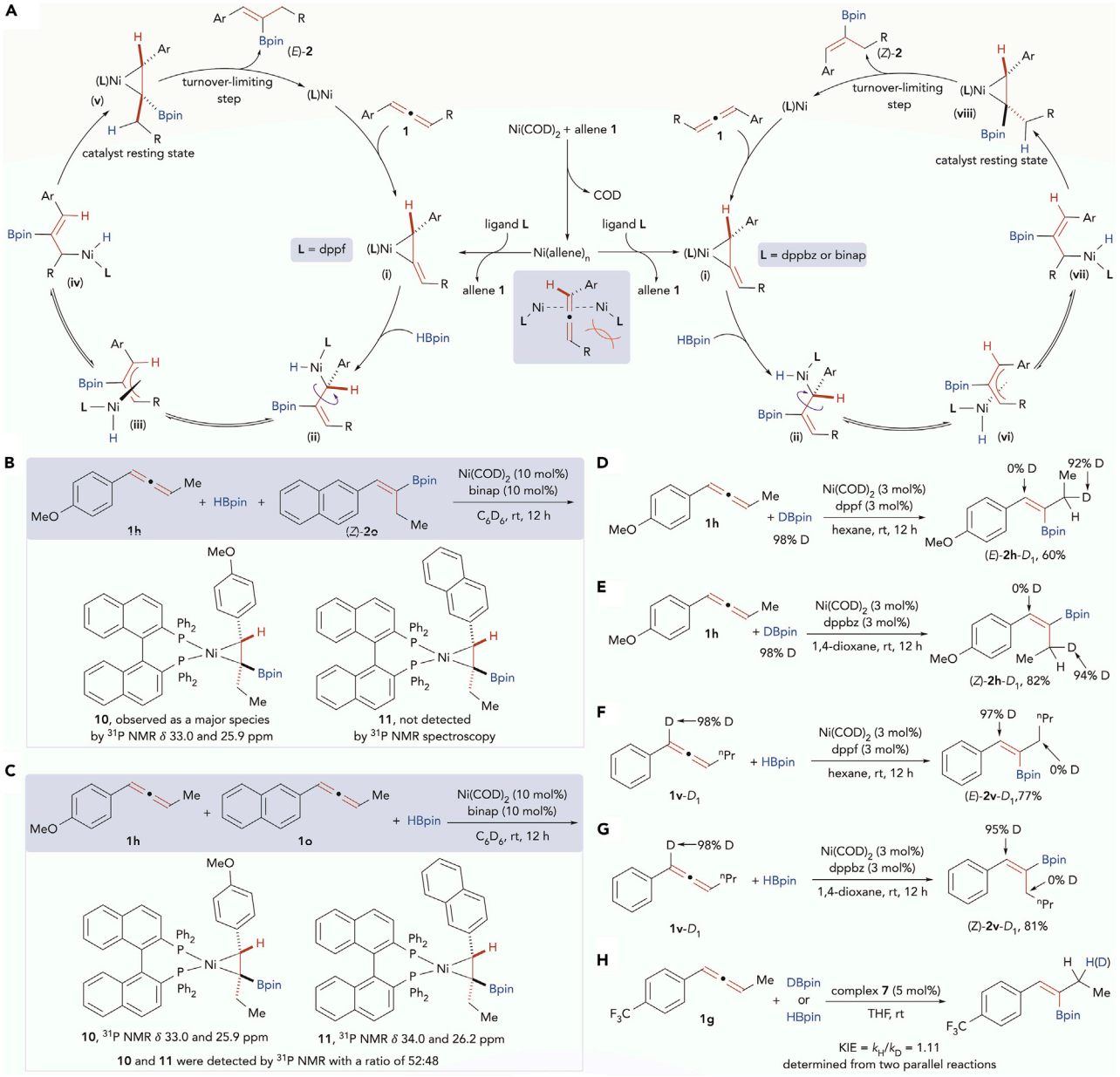

Figure 6. Mechanistic investigations

(A) Proposed reaction pathways for the nickel-catalyzed stereodivergent hydroboration reaction of allenes.

(B) Identifying nickel intermediates during $Ni(COD)_2$/binap-catalyzed hydroboration of allene **1h** in the presence of alkenylboronate (*Z*)-**2o** by ^{31}P NMR spectroscopy.

(C) Identifying nickel intermediates during $Ni(COD)_2$/binap-catalyzed hydroboration of a 1:1 mixture of allenes **1h** and **1o** by ^{31}P NMR spectroscopy.

(D) $Ni(COD)_2$/dppf-catalyzed hydroboration of allene **1h** with DBpin.

(E) $Ni(COD)_2$/dppbz-catalyzed hydroboration of allene **1h** with DBpin.

(F) $Ni(COD)_2$/dppf-catalyzed hydroboration of allene **1v**-d_1 with HBpin.

(G) $Ni(COD)_2$/dppbz-catalyzed hydroboration of allene **1v**-d_1 with HBpin.

(H) KIE experiment for the hydroboration of allene **1g** catalyzed by 5 mol % nickel-allene complex **7**.

(Figure 6C). Nickel-olefin complex **11** was not detected and nickel-olefin complex **10** was observed as the major nickel species for the reaction of allene **1h** in the presence of alkenylboronate (*Z*)-**2o** (Figure 6B). Nevertheless, both nickel-olefin complexes **10** and **11** were detected in a molar ratio of 52:48 during the hydroboration of a mixture

of allenes **1h** and **1o** (Figure 6C). These observations suggest that nickel-olefin intermediates formed during catalytic hydroboration reactions are generated from the association of alkenylboronate products, immediately after their formation through C–H reductive elimination, to the bisphosphine-ligated Ni(0) fragment without dissociation from the nickel center of the catalysts.

Deuterium-labeling experiments of hydroboration reactions with both nickel catalysts were also conducted to gain additional evidence to support the proposed reaction pathways, and the results are summarized in Figures 6D–6G. For example, hydroboration reactions of allene **1h** with DBpin catalyzed by $Ni(COD)_2$/dppf or $Ni(COD)_2$/dppbz yielded alkenylboronates (*E*)-**2h**-D_1 or (*Z*)-**2h**-D_1 in good yields, respectively (Figures 6D and 6E). The deuterium atoms are selectively incorporated onto the allylic carbon atoms. In addition, we also performed the reactions of allene **1v**-D_1 with HBpin in the presence of $Ni(COD)_2$/dppf or $Ni(COD)_2$/dppbz, and these two reactions afforded alkenylboronates (*E*)-**2v**-D_1 or (*Z*)-**2v**-D_1, with deuterium atoms solely located at the vinylic carbon atoms adjacent to the phenyl groups (Figures 6F and 6G). Furthermore, we measured the KIE value from two parallel reactions of allene **1h** with HBpin and DBpin catalyzed by nickel-allene complex **7** (Figure 6H), and a primary KIE of 1.11 suggests that HBpin is not involved in the turnover-limiting step of this nickel-catalyzed hydroboration reaction of allenes.

Synthetic utility

To highlight the synthetic utility of these nickel-catalyzed protocols, we first conducted gram-scale reactions of allene **1h** with HBpin to prepare alkenylboronates (*E*)-**2h** and (*Z*)-**2h**. The hydroboration of **1h** on a 6.0 mmol scale proceeded smoothly in the presence of 3 mol % $Ni(COD)_2$ and dppf and produced (*E*)-**2h** in 60% isolated yield (Figure 7A), and the corresponding reaction catalyzed by 3 mol % $Ni(COD)_2$ and dppbz afforded (*Z*)-**2h** in 80% isolated yield (Figure 7B). Second, we showed that these stereodefined alkenylboronates could undergo various transformations to yield other functionalized alkenes without loss of their stereochemistry. For example, protodeboronation of (*E*)-**2h** with KHF_2 afforded internal alkene (*E*)-**12** in high 89% isolated yield (Figure 7C).[52] Bromination[62] and iodination[52] of (*E*)-**2h** with NBS and I_2 formed alkenyl bromide (*Z*)-**13** and alkenyl iodide (*Z*)-**14** in 80% and 73% yields, respectively (Figures 7D and 7E). Alkenylboronate (*E*)-**2h** also underwent Pd-catalyzed Suzuki-Miyaura cross-coupling with 4-bromotoluene and 3-iodopyridine to produce di(hetero)aryl-substituted alkenes (*Z*)-**15** and (*Z*)-**16** in high 81% and 89% yields, respectively (Figures 7F and 7G).[20] Copper-catalyzed azidation of (*E*)-**2h** with NaN_3 afforded alkenylazide (*Z*)-**17** in 76% isolated yield (Figure 7H).[63] In addition, alkenylboronate (*E*)-**2h** also underwent Rh-catalyzed conjugated addition to chalcone to form carbonyl-functionalized trisubstituted alkene (*Z*)-**18** (Figure 7I).[64] Accordingly, protodeborylation, bromination, iodination, Suzuki-Miyaura coupling reactions, azidation, and conjugated addition to chalcone of alkenylboronate (*Z*)-**2h** afforded the corresponding functionalized alkene products (*Z*)-**12**, (*E*)-**13**, (*E*)-**14**, (*E*)-**15**, (*E*)-**16**, (*E*)-**17**, and (*E*)-**18** in high isolated yields (55%–91%), respectively (Figures 7C′–7I′). Therefore, these nickel-catalyzed stereodivergent hydroboration reactions of allenes provide a versatile foundation to access various stereodefined alkenyl compounds.

Conclusions

In summary, we have developed convenient and effective protocols to synthesize stereodefined trisubstituted *Z*- and *E*-alkenylboronates through ligand-controlled nickel-catalyzed stereodivergent hydroboration of allenes. A wide range of 1,3-disubstituted allenes reacted with HBpin in the presence of nickel catalysts generated *in situ* from $Ni(COD)_2$ and dppf or $Ni(COD)_2$ and dppbz, affording *E*- or *Z*-alkenylboronate

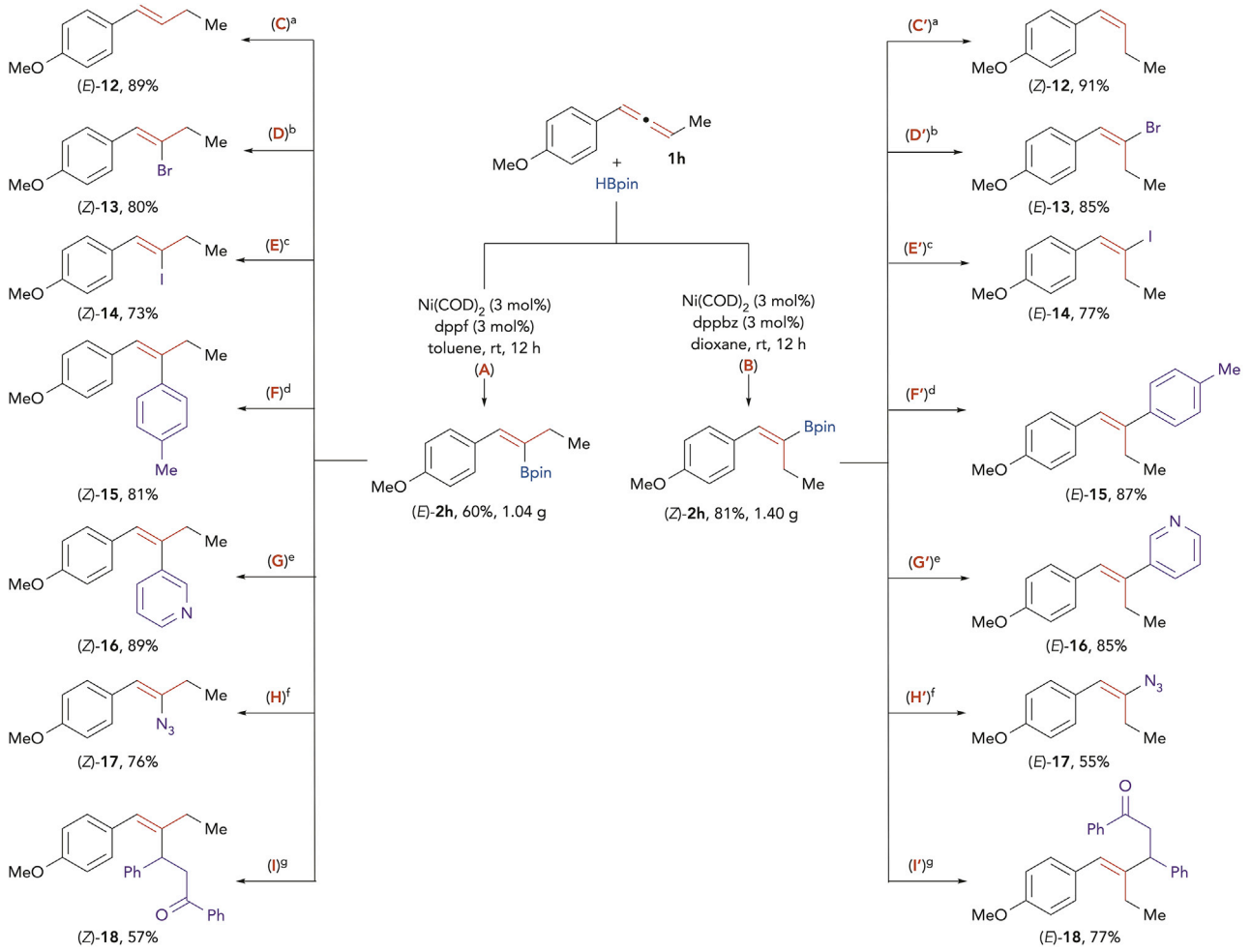

Figure 7. Synthetic applications of the nickel-catalyzed stereodivergent hydroboration reactions

(A) Gram-scale synthesis of (*E*)-**2h**.

(B) Gram-scale synthesis of (*Z*)-**2h**.

(C and C′) Protodeborylation of (*E*)-**2h** and (*Z*)-**2h**.

(D and D′) Bromination of (*E*)-**2h** and (*Z*)-**2h**.

(E and E′) Iodination of (*E*)-**2h** and (*Z*)-**2h**.

(F and F′) Suzuki-Miyaura coupling of (*E*)-**2h** and (*Z*)-**2h** with 4-bromotoluene.

(G and G′) Suzuki-Miyaura coupling of (*E*)-**2h** and (*Z*)-**2h** with 3-iodopyridine.

(H and H′) Azidation of (*E*)-**2h** and (*Z*)-**2h** with NaN_3.

(I and I′) Rh-catalyzed addition of (*E*)-**2h** and (*Z*)-**2h** to chalcone.

Reaction conditions: [a](*E*)-**2h** or (*Z*)-**2h** (0.200 mmol), KHF_2 (0.600 mmol), acetic acid (2 mL), room temperature, 12 h. [b](*E*)-**2h** or (*Z*)-**2h** (0.200 mmol), NBS (0.400 mmol), NaOH (aq, 3 M, 0.600 mmol), THF (1 mL), room temperature, 12 h. [c](*E*)-**2h** or (*Z*)-**2h** (0.200 mmol), I_2 (0.400 mmol), NaOH (aq, 3 M, 0.400 mmol), THF (1 mL), room temperature, 12 h. [d](*E*)-**2h** or (*Z*)-**2h** (0.200 mmol), $Pd(dba)_2$ (5 mol %), PPh_3 (20 mol %), K_3PO_4 (0.600 mmol), 4-bromotoluene (0.280 mmol), DMF (1 mL), 80°C, 12 h. [e](*E*)-**2h** or (*Z*)-**2h** (0.200 mmol), 3-iodopyridine (0.280 mmol), $Pd(dba)_2$ (5 mol %), PPh_3 (20 mol %), K_3PO_4 (0.600 mmol), DMF (1 mL), 80°C, 12 h. [f](*E*)-**2h** or (*Z*)-**2h** (0.200 mmol), NaN_3 (0.600 mmol), $CuSO_4$ (0.120 mmol), MeOH (1 mL), room temperature, 12 h. [g](E)-**2h** or (*Z*)-**2h** (0.200 mmol), chalcone (0.300 mmol), $[Rh(COD)Cl]_2$ (10 μmol), K_3PO_4 (0.300 mmol), 1,4-dioxane (1 mL), H_2O (0.4 mL), 80°C, and 12 h.

products in high yields with high stereoselectivity, respectively. To illustrate the pathways for these stereodivergent hydroboration reactions, several bisphosphine-ligated nickel-allene and nickel-olefin complexes have been synthesized and their competence as relevant nickel intermediates in these nickel-catalyzed allene hydroboration reactions has been verified. Instead of most frequently encountered ligation of $Ni(COD)_2$ with phosphine ligands, $Ni(COD)_2$ enters the catalytic cycle as a bisphosphine-ligated nickel-allene complex, which is formed through the replacement of

COD in $Ni(COD)_2$ with allenes followed by the coordination of bisphosphine ligands. The subsequent reaction of bisphosphine-ligated nickel-allene complex with HBpin to form the corresponding nickel-olefin complex is the stereo-determining step in these stereodivergent hydroboration reactions. Minimizing the steric interaction between bisphosphine and boryl-containing allyl ligands in allylnickel intermediates while maintaining the steric saturation around the nickel center controls the stereochemistry outcome of alkenylboronate products. This nickel-catalyzed stereodivergent hydroboration of allenes provides a versatile platform to access various types of stereodefined trisubstituted alkenyl compounds from readily accessible allene substrates with commercially available nickel catalysts.

EXPERIMENTAL PROCEDURES

Resource availability

Lead contact

Further information and requests for resources should be directed to and will be fulfilled by the lead contact, Shaozhong Ge (chmgsh@nus.edu.sg).

Materials availability

All materials generated in this study are available from the lead contact without restriction.

Data and code availability

All data needed to support the conclusions of this manuscript are included in the main text or supplemental information. Four data files for the X-ray crystal structures (CCDC: 2173388, 2173389, 2173392, and 2204151) have been deposited with the Cambridge Crystallographic Data Center and are available free of charge from www.ccdc.cam.ac.uk/data_request/cif or by emailing data_request@ccdc.cam.ac.uk, or by contacting the Cambridge Crystallographic Data Center, 12 Union Road, Cambridge CB2 1EZ, UK; fax: +44 1223 336033.

SUPPLEMENTAL INFORMATION

Supplemental information can be found online at https://doi.org/10.1016/j.chempr.2022.10.003.

ACKNOWLEDGMENTS

We thank Geok Kheng Tan and Irwan Iskandar Roslan for collecting the crystallographic data and solving the structures of nickel complexes **5**, **7**, **9**, and **10**. This work was supported by A*STAR under its AME IRG Grant (A20E5c0097).

AUTHOR CONTRIBUTIONS

S.G. directed the project, and X.Y. and C.Y. designed and performed the experimental work; S.G. and X.Y. co-wrote the manuscript. All authors contributed to the data analysis and the discussion.

DECLARATION OF INTERESTS

The authors declare no competing interests.

Received: May 25, 2022
Revised: August 29, 2022
Accepted: October 6, 2022
Published: November 2, 2022

REFERENCES

1. Itami, K., and Yoshida, J.-i. (2006). Multisubstituted olefins: Platform synthesis and applications to materials science and pharmaceutical chemistry. Bull. Chem. Soc. Jpn. *79*, 811–824.
2. Negishi, E., Wang, G., Rao, H., and Xu, Z. (2010). Alkyne elementometalation-Pd-catalyzed cross-coupling. Toward synthesis of all conceivable types of acyclic alkenes in high yields, efficiently, selectively, economically, and safely: "Green" way. J. Org. Chem. *75*, 3151–3182.
3. Lei, X., and Li, H. (2012). Selective alkene metathesis in the total synthesis of complex natural product. Top. Curr. Chem. *327*, 163–196.
4. Negishi, E., Huang, Z., Wang, G., Mohan, S., Wang, C., and Hattori, H. (2008). Recent advances in efficient and selective synthesis of di-, tri-, and tetrasubstituted alkenes via Pd-catalyzed alkenylation-carbonyl olefination synergy. Acc. Chem. Res. *41*, 1474–1485.
5. Siau, W.Y., Zhang, Y., and Zhao, Y. (2012). Stereoselective synthesis of *Z*-alkenes. Top. Curr. Chem. *327*, 33–58.
6. Eissen, M., and Lenoir, D. (2017). Mass efficiency of alkene syntheses with tri- and tetrasubstituted double bonds. ACS Sustainable Chem. Eng. *5*, 10459–10473.
7. Duan, X.F. (2020). Iron catalyzed stereoselective alkene synthesis: a sustainable pathway. Chem. Commun. *56*, 14937–14961.
8. Carreras, J., Caballero, A., and Pérez, P.J. (2019). Alkenyl boronates: Synthesis and applications. Chem. Asian J. *14*, 329–343.
9. Kovalenko, M., Yarmoliuk, D.V., Serhiichuk, D., Chernenko, D., Smyrnov, V., Breslavskyi, A., Hryshchuk, O.V., Kleban, I., Rassukana, Y., Tymtsunik, A.V., et al. (2019). The boron-Wittig olefination of aldehydes and ketones with bis[(pinacolato)boryl]methane: An extended reaction scope. Eur. J. Org. Chem. *2019*, 5624–5635.
10. Namirembe, S., Gao, C., Wexler, R.P., and Morken, J.P. (2019). Stereoselective synthesis of trisubstituted alkenylboron reagents by boron-Wittig reaction of ketones. Org. Lett. *21*, 4392–4394.
11. Cuenca, A.B., and Fernández, E. (2021). Boron-Wittig olefination with *gem*-bis(boryl)alkanes. Chem. Soc. Rev. *50*, 72–86.
12. Brown, H.C., and Bhat, N.G. (1988). A simple conversion of [*E*]- into the isomeric [*Z*]-2-(1-substituted-1-alkenyl)-1,3,2-dioxaborinanes, providing a convenient stereospecific synthesis of both [*E*]- and [*Z*]-1,2-disubstituted vinyl bromides. Tetrahedron Lett. *29*, 21–24.
13. Takagi, J., Takahashi, K., Ishiyama, T., and Miyaura, N. (2002). Palladium-catalyzed cross-coupling reaction of bis(pinacolato)diboron with 1-alkenyl halides or triflates: Convenient synthesis of unsymmetrical 1,3-dienes via the borylation-coupling sequence. J. Am. Chem. Soc. *124*, 8001–8006.
14. Gong, L., Li, C., Yuan, F., Liu, S., and Zeng, X. (2022). Chromium-catalyzed selective borylation of vinyl triflates and unactivated aryl carboxylic esters with pinacolborane. Org. Lett. *24*, 3227–3231.
15. Bismuto, A., Thomas, S.P., and Cowley, M.J. (2016). Aluminum hydride catalyzed hydroboration of alkynes. Angew. Chem. Int. Ed. *55*, 15356–15359.
16. Sang, H.L., Wu, C., Phua, G.G.D., and Ge, S. (2019). Cobalt-catalyzed regiodivergent stereoselective hydroboration of 1,3-diynes to access boryl-functionalized enynes. ACS Catal. *9*, 10109–10114.
17. Zhou, Y., You, W., Smith, K.B., and Brown, M.K. (2014). Copper-catalyzed cross-coupling of boronic esters with aryl iodides and application to the carboboration of alkynes and allenes. Angew. Chem. Int. Ed. *53*, 3475–3479.
18. Li, Z., and Sun, J. (2021). Copper-catalyzed 1,1-boroalkylation of terminal alkynes: access to alkenylboronates via a three-component reaction. Org. Lett. *23*, 3706–3711.
19. Sundararaju, B., and Fürstner, A. (2013). A trans-selective hydroboration of internal alkynes. Angew. Chem. Int. Ed. *52*, 14050–14054.
20. Kim, H.R., and Yun, J. (2011). Highly regio- and stereoselective synthesis of alkenylboronic esters by copper-catalyzed boron additions to disubstituted alkynes. Chem. Commun. *47*, 2943–2945.
21. Xu, S., Zhang, Y., Li, B., and Liu, S.Y. (2016). Site-selective and stereoselective *trans*-hydroboration of 1,3-enynes catalyzed by 1,4-azaborine-based phosphine-Pd complex. J. Am. Chem. Soc. *138*, 14566–14569.
22. Yuan, K., Suzuki, N., Mellerup, S.K., Wang, X., Yamaguchi, S., and Wang, S. (2016). Pyridyl directed catalyst-free *trans*-hydroboration of internal alkynes. Org. Lett. *18*, 720–723.
23. Alfaro, R., Parra, A., Alemán, J., García Ruano, J.L., and Tortosa, M. (2012). Copper(I)-catalyzed formal carboboration of alkynes: synthesis of tri- and tetrasubstituted vinylboronates. J. Am. Chem. Soc. *134*, 15165–15168.
24. Kondoh, A., and Jamison, T.F. (2010). Rhodium-catalyzed dehydrogenative borylation of cyclic alkenes. Chem. Commun. *46*, 907–909.
25. Selander, N., Willy, B., and Szabó, K.J. (2010). Selective C-H borylation of alkenes by palladium pincer complex catalyzed oxidative functionalization. Angew. Chem. Int. Ed. *49*, 4051–4053.
26. Reid, W.B., and Watson, D.A. (2018). Synthesis of trisubstituted alkenyl boronic esters from alkenes using the boryl-Heck reaction. Org. Lett. *20*, 6832–6835.
27. Wang, C., Wu, C., and Ge, S. (2016). Iron-catalyzed *E*-selective dehydrogenative borylation of vinylarenes with pinacolborane. ACS Catal. *6*, 7585–7589.
28. Ho, G.M., Segura, L., and Marek, I. (2020). Ru-catalyzed isomerization of ω-alkenylboronates towards stereoselective synthesis of vinylboronates with subsequent in situ functionalization. Chem. Sci. *11*, 5944–5949.
29. Xu, S., Geng, P., Li, Y., Liu, G., Zhang, L., Guo, Y., and Huang, Z. (2021). Pincer iron hydride complexes for alkene isomerization: catalytic approach to trisubstituted (*Z*)-alkenyl boronates. ACS Catal. *11*, 10138–10147.
30. Ping, Y., Wang, R., Wang, Q., Chang, T., Huo, J., Lei, M., and Wang, J. (2021). Synthesis of alkenylboronates from *N*-tosylhydrazones through palladium-catalyzed carbene migratory insertion. J. Am. Chem. Soc. *143*, 9769–9780.
31. Ohmura, T., Oshima, K., and Suginome, M. (2011). (E)- and (Z)-β-borylallylsilanes by alkyne silaboration followed by regio- and stereoselective double-bond migration. Angew. Chem. Int. Ed. *50*, 12501–12504.
32. Segura, L., Massad, I., Ogasawara, M., and Marek, I. (2021). Stereodivergent access to trisubstituted alkenylboronate esters through alkene isomerization. Org. Lett. *23*, 9194–9198.
33. Rej, S., Das, A., and Panda, T.K. (2021). Overview of regioselective and stereoselective catalytic hydroboration of alkynes. Adv. Synth. Catal. *363*, 4818–4840.
34. Hoffmann-Röder, A., and Krause, N. (2004). Synthesis and properties of allenic natural products and pharmaceuticals. Angew. Chem. Int. Ed. *43*, 1196–1216.
35. Krause, N., and Hashmi, A.S.K. (2004). Modern Allene Chemistry (Wiley).
36. Ma, S. (2005). Some typical advances in the synthetic applications of allenes. Chem. Rev. *105*, 2829–2872.
37. Yu, S., and Ma, S. (2012). Allenes in catalytic asymmetric synthesis and natural product syntheses. Angew. Chem. Int. Ed. *51*, 3074–3112.
38. Fujihara, T., and Tsuji, Y. (2018). Cu-catalyzed borylative and silylative transformations of allenes: Use of β-functionalized allyl copper intermediates in organic synthesis. Synthesis *50*, 1737–1749.
39. Thorpe, S.B., Guo, X., and Santos, W.L. (2011). Regio- and stereoselective copper-catalyzed β-borylation of allenoates by a preactivated diboron. Chem. Commun. *47*, 424–426.
40. Yuan, W., and Ma, S. (2012). Ligand controlled highly selective copper-catalyzed borylcuprations of allenes with bis(pinacolato) diboron. Adv. Synth. Catal. *354*, 1867–1872.
41. Semba, K., Fujihara, T., Terao, J., and Tsuji, Y. (2013). Copper-catalyzed borylation of α-alkoxy allenes with bis(pinacolato)diboron: Efficient synthesis of 2-boryl 1,3-butadienes. Angew. Chem. Int. Ed. *52*, 12400–12403.
42. Jang, H., Jung, B., and Hoveyda, A.H. (2014). Catalytic enantioselective protoboration of disubstituted allenes. Access to alkenylboron compounds in high enantiomeric purity. Org. Lett. *16*, 4658–4661.
43. Yuan, W., Song, L., and Ma, S. (2016). Copper-catalyzed borylcupration of allenylsilanes. Angew. Chem. Int. Ed. *55*, 3140–3143.
44. Zhu, C., Yang, B., Qiu, Y., and Bäckvall, J.E. (2016). Olefin-directed palladium-catalyzed

regio- and stereoselective hydroboration of allenes. Chem. Eur. J. *22*, 2939–2943.

45. Nagashima, Y., Sasaki, K., Suto, T., Sato, T., and Chida, N. (2018). Stereodivergent hydroboration of allenes. Chem. Asian J. *13*, 1024–1028.

46. Liu, J., Nie, M., Zhou, Q., Gao, S., Jiang, W., Chung, L.W., Tang, W., and Ding, K. (2017). Enantioselective palladium-catalyzed diboration of 1,1-disubstituted allenes. Chem. Sci. *8*, 5161–5165.

47. Szwetkowski, C., Slebodnick, C., and Santos, W.L. (2022). Regio- and stereoselective copper-catalyzed α,β-protoboration of allenoates: Access to *Z*-β,γ-unsaturated β-boryl esters. Org. Biomol. Chem. *20*, 3287–3291.

48. Yamamoto, Y., Fujikawa, R., Yamada, A., and Miyaura, N. (1999). A regio- and stereoselective platinum(0)-catalyzed hydroboration of allenes controlled by phosphine ligands. Chem. Lett. *28*, 1069–1070.

49. Semba, K., Shinomiya, M., Fujihara, T., Terao, J., and Tsuji, Y. (2013). Highly selective copper-catalyzed hydroboration of allenes and 1,3-dienes. Chem. Eur. J. *19*, 7125–7132.

50. Wu, C., and Ge, S. (2020). Ligand-controlled cobalt-catalyzed regiodivergent hydroboration of aryl,alkyl-disubstituted internal allenes. Chem. Sci. *11*, 2783–2789.

51. Li, C., Yang, Z., Wang, L., Guo, Y., Huang, Z., and Ma, S. (2020). Cobalt-catalyzed regio- and stereoselective hydroboration of allenes. Angew. Chem. Int. Ed. *59*, 6278–6283.

52. Yang, Y., Zeng, J.-H., and Zhan, Z.-P. (2021). Regio-divergent hydroboration of terminal allenes controlled by nickel and cobalt catalysts. Org. Chem. Front. *8*, 2537–2542.

53. Zhao, Y., and Ge, S. (2021). Chromium-catalyzed selective dimerization/hydroboration of allenes to access boryl-functionalized skipped (*E*,*Z*)-dienes. Angew. Chem. Int. Ed. *60*, 2149–2154.

54. Ge, S., and Hartwig, J.F. (2011). Nickel-catalyzed asymmetric α-arylation and heteroarylation of ketones with chloroarenes: Effect of halide on selectivity, oxidation state, and room-temperature reactions. J. Am. Chem. Soc. *133*, 16330–16333.

55. Yin, G., Kalvet, I., Englert, U., and Schoenebeck, F. (2015). Fundamental studies and development of nickel-catalyzed trifluoromethylthiolation of aryl chlorides: Active catalytic species and key roles of ligand and traceless MeCN additive revealed. J. Am. Chem. Soc. *137*, 4164–4172.

56. Greaves, M.E., Ronson, T.O., Lloyd-Jones, G.C., Maseras, F., Sproules, S., and Nelson, D.J. (2020). Unexpected nickel complex speciation unlocks alternative pathways for the reactions of alkyl halides with dppf-nickel(0). ACS Catal. *10*, 10717–10725.

57. Huang, Y., Ma, C., Liu, S., Yang, L.-C., Lan, Y., and Zhao, Y. (2021). Ligand coordination- and dissociation-induced divergent allylic alkylations using alkynes. Chem *7*, 812–826.

58. Touney, E.E., Van Hoveln, R., Buttke, C.T., Freidberg, M.D., Guzei, I.A., and Schomaker, J.M. (2016). Heteroleptic nickel complexes for the Markovnikov-selective hydroboration of styrenes. Organometallics *35*, 3436–3439.

59. Otsuka, S., and Nakamura, A. (1976). Acetylene and allene complexes: Their implication in homogeneous catalysis. Adv. Organomet. Chem. *14*, 245–283.

60. Lide, D.R. (2014). Molecular structure and spectroscopy. In CRC Handbook of Chemistry and Physics, Ninety-Fifth Edition, *9*, W.M. Haynes, ed (CRC Press), pp. 1–48.

61. Waterman, R. (2013). σ-Bond metathesis: A 30-year retrospective. Organometallics *32*, 7249–7263.

62. Bhavanarushi, S., Xu, Y., Khan, I., Luo, Z., Liu, B., and Xie, J. (2019). Transition-metal-free borylation of propargylic alcohols: Structurally variable synthesis in ionic liquid medium. Org. Chem. Front. *6*, 1895–1899.

63. Jayaram, V., Sridhar, T., Sharma, G.V.M., Berrée, F., and Carboni, B. (2018). Synthesis of polysubstituted isoquinolines and related fused pyridines from alkenylboronic esters via a copper-catalyzed azidation/aza-Wittig condensation sequence. J. Org. Chem. *83*, 843–853.

64. Sakai, M., Hayashi, H., and Miyaura, N. (1997). Rhodium-catalyzed conjugate addition of aryl- or 1-alkenylboronic acids to enones. Organometallics *16*, 4229–4231.